J|A|C|S
ARTICLES
Published on Web 04/23/2002

Discrimination between Peptide 3_{10}- and α-Helices. Theoretical Analysis of the Impact of α-Methyl Substitution on Experimental Spectra

Jan Kubelka, R. A. Gangani D. Silva, and Timothy A. Keiderling*

Contribution from the Department of Chemistry (M/C 111), University of Illinois at Chicago, 845 West Taylor Street, Chicago, Illinois 60607-7061

Received December 10, 2001

Abstract: Detailed spectral simulations based on ab initio density functional theory computations of the amide I and II infrared (IR) and vibrational circular dichroism (VCD) spectra for Ac−$(Ala)_4$−NH_2, Ac−$(Aib\text{-}Ala)_2$−NH_2, and Ac−$(Aib)_4$−NH_2 constrained to 3_{10}- and α-helical conformations are presented. Parameters from these ab initio calculations are transferred onto corresponding larger oligopeptides to simulate the spectra for dodecamers. The differences between conformations and for different Aib substitution patterns within a conformation are reflected in observable spectral patterns where data are available. Simulated IR spectra show small frequency shifts in the amide I maxima between 3_{10}- and α-helices, but the same magnitude shifts occur within one conformation upon Aib substitution. Thus, from a computational basis, the frequency of the amide I maximum does not discriminate between the 3_{10}- or α-helical conformations. Calculated VCD band shapes for 3_{10}-helices showed more significant changes in amplitude, with change in the fraction of Aib, than those for α-helices. Generally, with increasing Aib content, the overall amide I VCD intensity becomes weaker and the amide I couplet becomes more conservative, while the amide II VCD is less affected. Although the detailed band shape is shown to be sensitive to α-Me substitution, the basic pattern of amide I and II relative VCD intensities still differs between α- and 3_{10}-helices and, as a consequence, successfully discriminates between them. These predictions are all borne out in experimental spectra of Aib, mixed Aib−Ala, and Ala-based helical peptides, where available.

Introduction

The 3_{10}-helix is an important component of protein secondary structure[1,2] and commonly occurs in peptides rich in $C^{\alpha,\alpha}$-disubstituted α-amino acids (for example, containing α,α-dimethylglycine or aminoisobutyric acid, Aib).[3−10] However, distinguishing 3_{10}-helices from α-helices by use of spectral band shapes has been the subject of some debate.[11−15] Several years ago we empirically demonstrated that vibrational circular dichroism (VCD) spectra of the amide I and II transitions for some model 3_{10}-helices yielded a unique intensity pattern.[16,17] While both 3_{10}- and α-conformers yield the same overall sign of the VCD band shapes, the detailed shapes differ, and most importantly, the amide I and II bands have different relative intensities.

Somewhat later, a number of reports appeared claiming to assign an infrared (IR) amide I′ absorption component found at ∼1639 cm^{-1}, significantly lower than that for α-helices, to the 3_{10}-helical contribution for some proteins dissolved in D_2O.[18−20] While the model peptide spectra did not support this assignment,[21] there were important differences between the model peptide and protein studies. First, the proteins were in aqueous solution, potentially involving hydrogen bonding of the D_2O solvent to the 3_{10}-helices, which might shift their amide I′ frequency, but the model 3_{10}-helical peptides then available were not water soluble. It is now known that the traditional IR amide I frequency marker for α-helices in peptides can change significantly depending on local environment. Truncation of the

* To whom correspondence should be addressed. Phone: (312) 996-3156. Fax: (312) 996-0431. E-mail: tak@uic.edu.

(1) Barlow, D. J.; Thornton, J. M. *J. Mol. Biol.* **1988**, *201*, 601.
(2) Bolin, K. A.; Millhauser, G. L. *Acc. Chem. Res.* **1999**, *32*, 1027.
(3) Toniolo, C.; Benedetti, E. *Macromolecules* **1991**, *24*, 4004.
(4) Toniolo, C.; Crisma, M.; Formaggio, F.; Valle, G.; Cavicchioni, G.; Precigoux, G.; Aubry, A.; Kamphius, J. *Biopolymers* **1993**, *33*, 1601.
(5) Toniolo, C.; Benedetti, E. *Trends Biol. Sci.* **1991**, *16*, 350.
(6) Karle, I. L.; Balaram, P. *Biochemistry* **1990**, *29*, 6747.
(7) Tirado-Rives, J.; Maxwell, D. S.; Jorgensen, W. L. *J. Am. Chem. Soc.* **1993**, *115*, 11590.
(8) Zhang, L.; Hermans, J. *J. Am. Chem. Soc.* **1994**, *116*, 11915.
(9) Smythe, M. L.; Nakaie, C. R.; Marshall, G. R. *J. Am. Chem. Soc.* **1995**, *117*, 10555.
(10) Yokum, T. S.; Gauthier, T. J.; Hammer, R. P.; McLaughlin, M. L. *J. Am. Chem. Soc.* **1997**, *119*, 1167.
(11) Toniolo, C.; Polese, A.; Formaggio, F.; Crisma, M.; Kamphuis, J. *J. Am. Chem. Soc.* **1996**, *118*, 2744.
(12) Yoder, G.; Polese, A.; Silva, R. A. G. D.; Formaggio, F.; Crisma, M.; Broxterman, Q. B.; Kamphuis, J.; Toniolo, C.; Keiderling, T. A. *J. Am. Chem. Soc.* **1997**, *119*, 10278.
(13) Manning, M. C.; Woody, R. W. *Biopolymers* **1991**, *31*, 569.
(14) Vijayakumar, E. K. S.; Sudha, T. S.; Balaram, P. *Biolopymers* **1984**, *23*, 877.
(15) Anderson, N. H.; Liu, Z.; Prickett, K. S. *FEBS Lett.* **1996**, *399*, 47.
(16) Yasui, S. C.; Keiderling, T. A.; Bonora, G. M.; Toniolo, C. *Biopolymers* **1986**, *25*, 79.
(17) Yasui, S. C.; Keiderling, T. A.; Formaggio, F.; Bonora, G. M.; Toniolo, C. *J. Am. Chem. Soc.* **1986**, *108*, 4988.
(18) Haris, P. I.; Chapman, D. *Biochim. Biophys. Acta* **1988**, *943*, 375.
(19) Holloway, P. W.; Mantsch, H. H. *Biochemistry* **1989**, *28*, 931.
(20) Prestrelski, S. J.; Byler, D. M.; Thompson, M. P. *Int. J. Pept. Protein Res.* **1991**, *37*, 508.
(21) Kennedy, D. F.; Crisma, M.; Toniolo, C.; Chapman, D. *Biochemistry* **1991**, *30*, 6541.

helices leads to an intensity redistribution in the band with components covering a relatively wide interval (>30 cm^{-1}).[22−25] More importantly, solvated α-helices, particularly for isolated single peptides in D_2O, can have unusually low-frequency IR transitions (~1637 cm^{-1}).[26−30] These both may explain the low frequencies assigned to distorted helices in some proteins,[31−33] which may be attributable to solvated helices such as those on the surface of the fold.[27,28] Additionally, it opens the possibility that a solvated aqueous 3_{10}-helix could have a relatively large frequency shift from that characteristic of nonaqueous 3_{10}-helices (~1660 cm^{-1}). Thus far a precise comparison has not been possible, since no stable isolated 3_{10}-helices soluble in aqueous solutions were known. Recently, however, this synthetic problem has been resolved.[10,34]

Second, H/D exchange might also shift the frequency. For α-helical model peptides and proteins, the amide I/I′ frequency difference is relatively small, 4−5 cm^{-1}. The proposed assignment would suggest much larger frequency shifts due to N-deuteration for 3_{10}-helices.[20,35,36] However, α-Me-based model studies in nonaqueous solvents did not support this observation.[21]

Third, all the 3_{10}-model systems studied to date employed some fraction of residues with α-Me (or equivalent) substitution to attain stability, yet 3_{10}-helices in proteins are composed of "normal" amino acids. The question thus arises whether the VCD band shape signature proposed to be specific for the 3_{10}-helix is merely a consequence of the perturbation of the vibrational states caused by α-methylation. This question is addressed in the present study. While short peptides of proteinic residues cannot form stable 3_{10}- or α-helices, one can stabilize them in a computational experiment and can thereby investigate the impact of α-Me residues on the resulting IR and VCD spectra for either 3_{10}- or α-helical structures. Such computations can then be undertaken for any mix of normal (i.e., Ala) and α-Me (i.e., Aib) residues for any structure, or even a mix of structures.

Theoretical spectral simulations using the ab initio quantum mechanical magnetic field perturbation (MFP) method[37,38] for model Ala-based peptide structures have reflected the relative change in the amide I − amide II VCD intensity difference between 3_{10}- and α-helices.[25,39] The spectral property tensors (force field, FF, atomic polar and axial tensors, APT and AAT) obtained from these ab initio calculations can also be transferred onto much longer oligopeptide models for simulation of IR and VCD spectra for longer, more uniform polymers.[30,39,40] Simulations based on dipeptide and longer peptide MFP computations support the contention that the qualitative differences (relative amide I − amide II VCD) between the 3_{10}- and α-helical VCD patterns arise primarily from the interaction of near-neighbor amides (local ϕ, ψ conformational angles), being qualitatively consistent with length variation and roughly independent of side-chain interactions.[25,39,41] These theoretical calculations are another way of demonstrating the relatively local, short-range interaction spectral dependence of VCD.[17,42−46]

Vibrational frequency calculations based on empirical force fields were previously carried out for poly-Aib in α-helical and 3_{10}-helical conformations by Dwivedi et al.[35] To determine the effect of the α-methylated residues, the α-helical poly-Aib results were compared to those for α-helical poly(L-Ala).[47] While the 3_{10}-helical poly-Aib was predicted to have higher amide I and II frequencies than the α-helical form, no difference in the frequencies of these bands was predicted between the α-helical poly-Aib and poly(L-Ala).[47] However, to our knowledge no computations have been reported comparing the impact of incorporating Aib or a mix of Aib and Ala residues on peptide VCD spectra, and particularly, no ab initio IR and VCD calculations have been reported for such sequences in these two helical structures. Below we present the first such ab initio quantum mechanically based IR and VCD calculations for peptides explicitly containing Aib residues, as opposed to Ala (or Gly), which were the residues used for previous theoretical simulations.[25,30,39,41] It should be noted that a method for distinguishing 3_{10}- from α-helices using electronic CD (ECD) in the UV has been proposed.[11,13] While this works fairly well for α-Me-substituted peptides, it loses generality with mixed sequences, as will be demonstrated in detail in a separate publication.[48]

Materials and Methods

Calculational Methods. The simulations of IR and VCD spectra were based on quantum mechanical force fields, atomic polar and axial tensors, calculated at the density functional (DFT) BPW91/6-31G* level, using the Gaussian 98 program package. The AAT calculation has been implemented in Gaussian 98 at both HF and DFT levels[38] according to the MFP theory of Stephens,[37] and with gauge including atomic orbitals (GIAO) to ensure gauge invariance.[38,49] The BPW91/6-31G* level was used, as in our previous computational studies,[25,30,39] since it seems to provide the best tradeoff of performance and computational cost as compared to other common pure and hybrid density functional methods with the same and even larger basis sets.[25,50] The DFT calculations were carried out for the model peptides Ac−

(22) Torii, H.; Tasumi, M. *J. Chem. Phys.* **1992**, *96*, 3379.
(23) Krimm, S.; Reisdorf, W. C., Jr. *Faraday Discuss.* **1994**, *99*, 181.
(24) Nevskaya, N. A.; Chirgadze, Y. N. *Biopolymers* **1976**, *15*, 637.
(25) Kubelka, J.; Silva, R. A. G. D.; Bour, P.; Decatur, S. M.; Keiderling, T. A. In *Chirality: Physical Chemistry*; ACS Symposium Series 810; Hicks, J. M., Ed.; American Chemicsl Society: Washington, DC, 2002; p 50.
(26) Haris, P. I.; Chapman, D. *Biopolymers* **1995**, *37*, 251.
(27) Martinez, G.; Millhauser, G. *J. Struct. Biol.* **1995**, *114*, 23.
(28) Williams, S.; Causgrove, T. P.; Gilmanshin, R.; Fang, K. S.; Callender, R. H.; Woodruff, W. H.; Dyer, R. B. *Biochemistry* **1996**, *35*, 691.
(29) Yoder, G.; Pancoska, P.; Keiderling, T. A. *Biochemistry* **1997**, *36*, 15123.
(30) Silva, R. A. G. D.; Kubelka, J.; Decatur, S. M.; Bour, P.; Keiderling, T. A. *Proc. Natl. Acad. Sci. U.S.A.* **2000**, *97*, 8318.
(31) Trewhella, J.; Liddle, W. K.; Heidorn, D. B.; Strynadka, N. *Biochemistry* **1989**, *28*, 1294
(32) Dousseau, F.; Pezolet, M. *Biochemistry* **1990**, *29*, 8771.
(33) Jackson, M.; Haris, P. I.; Chapman, D. *Biochemistry* **1991**, *30*, 9681.
(34) Formaggio, F.; Crisma, M.; Rossi, P.; Scrimin, P.; Kaptein, B.; Broxterman, Q. B.; Kamphuis, J.; Toniolo, C. *Chem. A Eur. J.* **2000**, *6*, 4498.
(35) Dwivedi, A. M.; Krimm, S.; Malcolm, B. R. *Biopolymers* **1984**, *23*, 2025.
(36) Miick, S. M.; Martinez, G.; Fiori, W. R.; Todd, A. P.; Millhauser, G. L. *Nature* **1992**, *359*, 653.
(37) Stephens, P. J. *J. Phys. Chem.* **1985**, *89*, 748.
(38) Stephens, P. J.; Ashvar, C. S.; Devlin, F. J.; Cheeseman, J. R.; Frisch, M. J. *Mol. Phys.* **1996**, *89*, 579.
(39) Bour, P.; Kubelka, J.; Keiderling, T. A. *Biopolymers* **2000**, *53*, 380.
(40) Bour, P.; Sopkova, J.; Bednarova, L.; Malon, P.; Keiderling, T. A. *J. Comput. Chem.* **1997**, *18*, 646.
(41) Bour, P.; Keiderling, T. A. *J. Am. Chem. Soc.* **1993**, *115*, 9602.
(42) Dukor, R. K.; Keiderling, T. A.; Gut, V. *Int. J. Pept. Protein Res.* **1991**, *38*, 198.
(43) Dukor, R. K.; Keiderling, T. A. *Biopolymers* **1991**, *31*, 1747.
(44) Keiderling, T. A.; Pancoska, P. In *Biomolecular Spectroscopy, Part B*; Hester, R. E., Clarke, R. J. H., Eds.; Wiley: Chichester, 1993; Vol. 21, p 267.
(45) Mastle, W.; Dukor, R. K.; Yoder, G.; Keiderling, T. A. *Biopolymers* **1995**, *36*, 623.
(46) Yoder, G.; Keiderling, T. A.; Formaggio, F.; Crisma, M.; Toniolo, C. *Biopolymers* **1995**, *35*, 103.
(47) Krimm, S.; Bandekar, J. *Adv. Protein Chem.* **1986**, *38*, 181.
(48) Silva, R. A. G. D.; Yasui, S. C.; Kubelka, J.; Formaggio, F.; Crisma, M.; Toniolo, C.; Keiderling, T. A.,submitted for publication.
(49) Bak, K. L.; Jorgensen, P.; Helgaker, T.; Ruud, K.; Jensen, H. J. *J. Chem. Phys.* **1993**, *98*, 8873.
(50) Kubelka, J.; Keiderling, T. A. *J. Phys. Chem. A* **2001**, *105*, 10922.

$(Ala)_4-NH_2$, $Ac-(Aib-Ala)_2-NH_2$, and $Ac-(Aib)_4-NH_2$ as 3_{10}-helices and $Ac-(Ala)_6-NH_2$ and $Ac-(Aib-Ala)_3-NH_2$, in the α-helical conformation. Such 5- and 7-amide-containing peptide models for 3_{10}- and α-helices, respectively, were chosen to contain a central amide group with a fully developed intramolecular H-bonding pattern characteristic for the conformation. These structures were constrained to maintain standard ϕ, ψ, and ω values corresponding to the 3_{10}-helical ($\phi = -60°$, $\psi = -30°$, $\omega = 180°$) and α-helical ($\phi = -57°$, $\psi = -47°$, $\omega = 180°$) conformations, while all other geometry parameters were fully optimized prior to each force field and spectral intensity parameter calculation.

The spectral parameters for larger dodecapeptides, $Ac-(Ala)_{12}-NH_2$, $Ac-(Aib-Ala)_6-NH_2$, and $Ac-(Aib)_{12}-NH_2$ in 3_{10}-helical, and the first two also in α-helical conformations, were obtained through transfer of the ab initio FF, APT, and AAT values from the corresponding smaller oligopeptides by use of the property-transfer method of Bour et al.[40] The computed interference of the $-CH_3$ group vibrations with the amide II VCD, was eliminated by substituting deuterium for all methyl hydrogens.[25,39] (Without this, the mode structure is exceptionally complex due to the DFT FF computed $-CH_3$ deformations being too high and amide II too low in frequency when isolated molecule calculations are compared to solution data.[50] However, tests with and without this $-CD_3$ substitution yield the same amide I and II VCD pattern.) Parameter transfer, isotopic substitutions, and frequency and intensity calculations were done using our own programs.[25,40] The resultant IR and VCD band shapes were obtained in all cases by summing over normal modes represented by Lorentzian bands having widths of 20 cm^{-1} and areas proportional to the dipolar (D) or rotational (R) strengths for IR and VCD simulations, respectively.

Comparison Data. Computational results are here compared with experimental data that have been previously reported by our laboratory for a number of blocked peptides. Those 3_{10}-helical and mixed helical peptides containing Aib or other α-Me-substituted residues were obtained from Prof. Claudio Toniolo, University of Padova.[12,17,46,48,51] Some α-helical model peptides were obtained from Prof. R. Katachai, Dr. A. Brack, Dr. C. A. Rohl, and Prof. R. A. Baldwin,[29,52,53] and others were obtained commercially.[54−56]

Results

The fully ab initio simulated VCD and IR spectra for the amide I and II bands for three tetramer peptides, $Ac\text{-}Aib_4-NH_2$, $Ac-(Aib-Ala)_2-NH_2$, and $Ac-Ala_4-NH_2$, in a 3_{10}-helical conformation, are shown in Figure 1. (While all the normal modes are calculated with our method, only the amides I and II have been used empirically for the 3_{10}-helix discrimination question addressed in this paper.) Clearly, the qualitative IR pattern is stable for these sequences, differing primarily with regard to the frequencies and relative intensities for components of each band. Some structure is evident in the amide I IR band shape, but the largest shifts from the main band are for the unique amides, i.e., the C-terminal, non-H-bonded carbonyl group (high-frequency sideband) and the N-blocking acetoamide group (low-frequency shoulder). These components naturally become relatively less important in longer peptides, which effects a sharpening of the predicted transitions (see below). The all-Ala peptide has its amide I absorption maximum higher in frequency (by ~10 cm^{-1}) than for the other two peptides, which have maxima at approximately the same frequency. The amide II band is similar for all sequences, with minor differences in the component separation (especially for Aib−Ala) but not in their relative intensity distribution. The most intense amide II component approaches the most intense amide I component IR intensity. The amide I and II vibrational frequencies, both simulated and experimental, are summarized in Table 1 for easier reference.

Similarly, the basic pattern of positive couplet VCD for the amide I and intense negative VCD for the amide II is

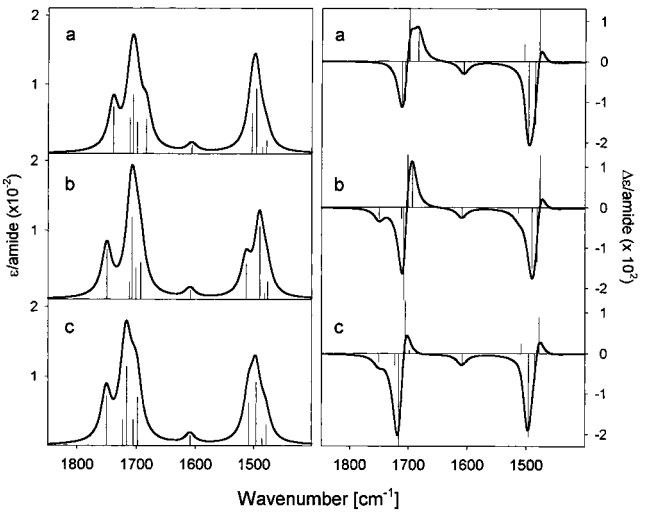

Figure 1. Ab initio simulated amide I and amide II IR (left) and VCD (right) spectra for three tetrapeptides with different distributions of α-methylated residues, all constrained to the 3_{10}-helical conformation ($\phi = -60°$, $\psi = -30°$, $\omega = 180°$): (a) $Ac-(Aib)_4-NH_2$; (b) $Ac-(Aib-Ala)_2-NH_2$; (c) $Ac-(Ala)_4-NH_2$.

Table 1. Summary of Calculated and Experimental Amide I and II Band Frequencies (ν_{max}) and VCD Intensities ($\Delta A/A_{max}$)[a]

		amide I		amide II	
peptide[b]	structure	ν_{max} (cm^{-1})	$\Delta A/A_{max}$ ($\times 10^5$)	ν_{max} (cm^{-1})	$\Delta A/A_{max}$ ($\times 10^5$)
Calculated Band Frequencies					
DFT BPW91/6-31G*					
$Ac-(Aib)_4-NH_2$	3_{10}-helix	1706	12	1499	12
$Ac-(Aib-Ala)_2-NH_2$	3_{10}-helix	1707	14	1491	10
$Ac-(Ala)_4-NH_2$	3_{10}-helix	1717	14	1498	11
$Ac-(Aib-Ala)_3-NH_2$	α-helix	1718	21	1508	8
$Ac-(Ala)_6-NH_2$	α-helix	1724	20	1511	6
parameter transfer					
$Ac-(Aib)_{12}-NH_2$	3_{10}-helix	1706	17	1507	17
$Ac-(Aib-Ala)_6-NH_2$	3_{10}-helix	1705	15	1516	11
$Ac-(Ala)_{12}-NH_2$	3_{10}-helix	1713	15	1514	12
$Ac-(Aib-Ala)_6-NH_2$	α-helix	1713	22	1515	8
$Ac-(Ala)_{12}-NH_2$	α-helix	1719	20	1516	6
Experimental Band Frequencies					
poly(Aib)/dry film[c]	3_{10}-helix	1656	−	1545	
$Z\text{-}Aib_5-Leu-Aib_2-OMe/CDCl_3$[d]	3_{10}-helix	1663	14	1531	14
$Z\text{-}(Aib-Ala)_4-OMe/CDCl_3$[e]	3_{10}-helix	1664	15	1533	11
$(Met_2-Leu)_6/CDCl_3$[f]	α-helix	1654	23	1545	7
poly(γ-benzyl−Glu)/$CDCl_3$[g]	α-helix	1652	23	1550	8
$Z\text{-}(\alpha Me-Val)_8-OMe/TFE$[h]	3_{10}-helix	1658	11	1533	9
$Z\text{-}(Aib-Ala)_4-OMe/TFE$[e]	3_{10}-helix	1663	11	1538	10
$Ac-(Ala_2-Lys-Ala_2)_3-Gly-Tyr\text{-}NH_2/TFE$[i]	α-helix	1660	20	1550	12

[a] Ratio of peak-to-peak differential absorbance (ΔA) to peak amide I absorbance A_{max}. [b] All natural amino acids L-. [c] References 35 and 47. [d] References 16 and 17. [e] References 48 and 57. [f] Reference 52. [g] References 56, 60, and 61. [h] Reference 12. [i] References 29 and 58.

(51) Yoder, G.; Keiderling, T. A.; Formaggio, F.; Crisma, M. *Tetrahedron Asymmetry* **1995**, *6*, 687.
(52) Yasui, S. C.; Keiderling, T. A.; Katachai, R. *Biopolymers* **1987**, *26*, 1407.
(53) Baumruk, V.; Huo, D. F.; Dukor, R. K.; Keiderling, T. A.; Lelievre, D.; Brack, A. *Biopolymers* **1994**, *34*, 1115.
(54) Sen, A. C.; Keiderling, T. A. *Biopolymers* **1984**, *23*, 1533.
(55) Yasui, S. C.; Keiderling, T. A. *Biopolymers* **1986**, *25*, 5.
(56) Malon, P.; Kobrinskaya, R.; Keiderling, T. A. *Biopolymers* **1988**, *27*, 733.

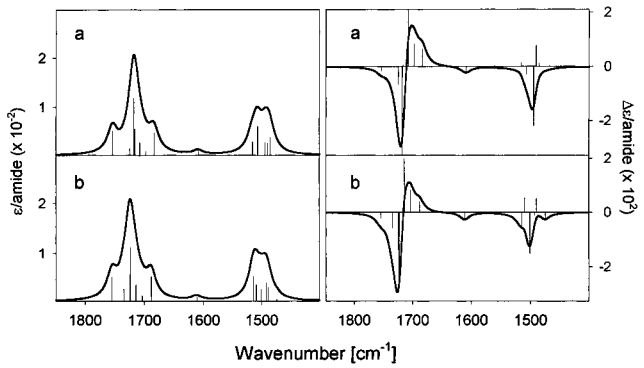

Figure 2. Ab initio simulated amide I and amide II IR (left) and VCD (right) spectra for two hexapeptides with and without α-methylated residues, both constrained to the same α-helical conformation ($\phi = -57°$, $\psi = -47°$, $\omega = 180°$): (a) Ac−(Aib−Ala)$_3$−NH$_2$; (b) Ac−(Ala)$_6$−NH$_2$.

characteristic of all three oligomers, no matter what amount of Aib is present. However, details of the band shapes vary, most dramatically for the amide I VCD couplet. The effect of changing Aib to Ala is reflected in a predicted increase in the intensity of the negative VCD component of the amide I band relative to that of the amide II. The balance between positive and negative lobes in the amide I VCD couplet thereby shifts with reduced C-methylated (Aib) content to favor the negative lobe. This could have importance for characterizing 3_{10}-helices with proteinic residues. The amide II VCD has only minor variations with sequence change in both the overall band shape and intensity.

For comparison, the ab initio simulated amide I and II IR and VCD spectra for α-helical hexapeptides Ac−(Aib-Ala)$_3$−NH$_2$ and Ac−Ala$_6$−NH$_2$ are shown in Figure 2. The α-helical amide I IR maximum shows a systematic small shift to a higher frequency for both the −Aib−Ala− and −Ala− sequences, by ∼6 and ∼8 cm^{-1}, respectively, as compared to the 3_{10}-helix (Table 1). The amide I frequency for the α-helical all-Ala peptide is again higher than for the α-helical −Ala−Aib− peptide, but in this case only by ∼5 cm^{-1}. The low-frequency amide I components in the α-helical simulated IR spectra overlap the absorption maxima for the corresponding 3_{10}-helical sequences, a property that would inhibit analysis of mixed conformations by IR alone. The α-helical amide II IR bands are not observably shifted in frequency from the corresponding 3_{10}-helical computations. Several components have nearly the same intensity results in an overall broadened shape for the α-helical amide II, with about half of the amide I IR peak intensity. Again, the VCD of these peptides show typical α-helical band shapes for both sequences. The amide I VCD is more intense, by a factor of ∼2, than is the 3_{10}-helical amide I VCD and is negatively biased. The α-helical amide II VCD, on the other hand, is weaker and broader than its amide I VCD and much weaker than the 3_{10} amide II. The difference between the two sequences is smaller for the α-helical than for the 3_{10}-helical case above.

To test the variations with peptide size, the fully ab initio DFT-MFP parameters from the model peptides above were propagated onto corresponding longer peptides Ac−Aib$_{12}$−NH$_2$ (3_{10}-helix), and Ac−(Aib-Ala)$_6$−NH$_2$ and Ac−Ala$_{12}$−NH$_2$ (3_{10}- and α-helix), using the Cartesian property tensor-transfer method.[40] The resulting simulated spectra for the 3_{10}-helical dodecapeptides are shown in Figure 3 and for the α-helical

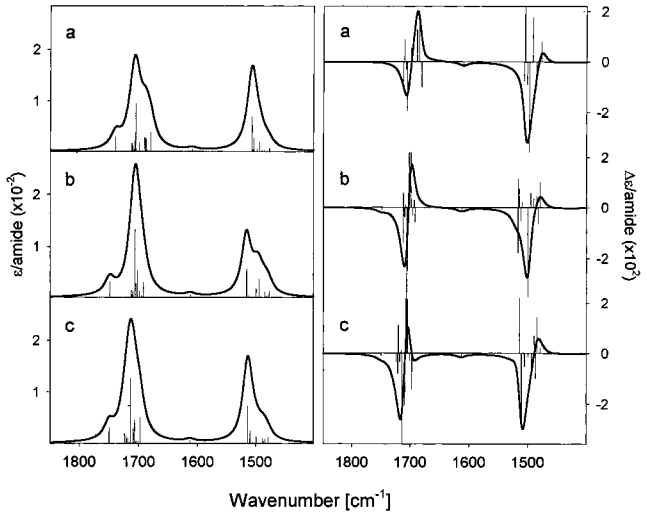

Figure 3. Simulated IR (left) and VCD (right) spectra for three 3_{10}-helical dodecapeptides with different distributions of α-methylated residues: (a) Ac−(Aib)$_{12}$−NH$_2$; (b) Ac−(Aib-Ala)$_6$−NH$_2$; (c) Ac−(Ala)$_{12}$−NH$_2$. Spectra were simulated by transfer of ab initio parameters calculated for the shorter peptides in Figure 1. Conformational parameters are the same as in Figure 1.

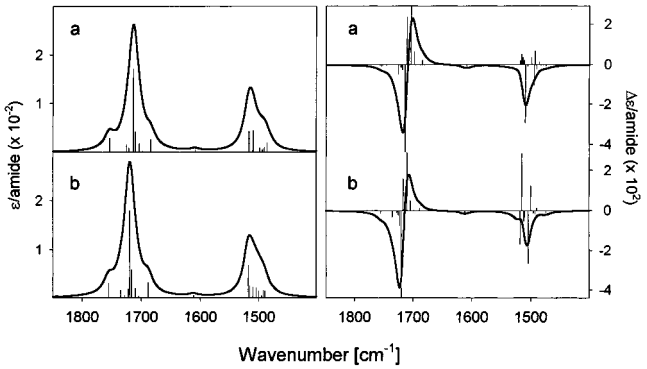

Figure 4. Simulated IR (left) and VCD (right) spectra for two α-helical dodecapeptides with and without α-methylated residues: (a) Ac−(Aib−Ala)$_6$−NH$_2$; (b) Ac−(Ala)$_{12}$−NH$_2$. Spectra were simulated by transfer of ab initio parameters calculated for the shorter models in Figure 2. Conformational parameters are the same as in Figure 2.

dodecapeptides in Figure 4. Qualitatively, the trends in these IR and VCD spectral band shapes simulated for longer peptides with transferred parameters are the same as those computed ab initio for the shorter models, thus indicating that there is no significant length dependence in the fundamental spectral properties at this level of theory. This is consistent with our previous computations for α-helices where simulated spectra for peptides as long as Ac−Ala$_{20}$−NH$_2$ corresponded to those in Figure 4.[25,30] The low- and high-frequency amide I components associated with the end residues have a smaller contribution to the overall band shape; thus, both the IR and VCD amide I and II band shapes are more uniform, and more sharply peaked, but the frequencies of the absorption maxima did not change from the shorter peptide result (Table 1). This narrowing has a bigger impact on the α-helical than on the 3_{10}-helical spectra.

The longer 3_{10}-helices (Figure 3) again show a positive couplet amide I that is in all cases weaker than the associated strong negative amide II VCD, making the distinction between the 3_{10}- and α-helical (Figure 4) VCD patterns perhaps even more obvious than in the shorter oligopeptides. In both cases, the sharpening of the absorption band is accompanied by

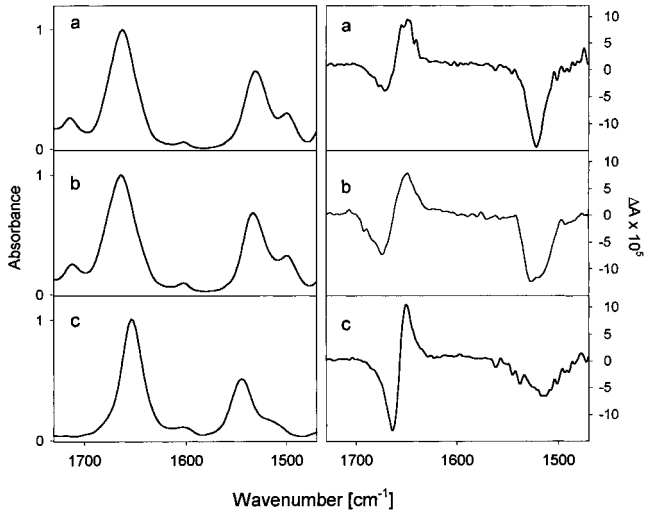

Figure 5. Experimental IR (left) and VCD (right) spectra for three model helical peptides with different fraction of α-methylated residues, measured in $CDCl_3$ solutions: (a) 3_{10}-helical Z-Aib_5−L-Leu−Aib_2−OMe; (b) 3_{10}-helical Z-(Aib−Ala)$_3$−OMe; (c) α-helical $(Met_2-Leu)_6$.

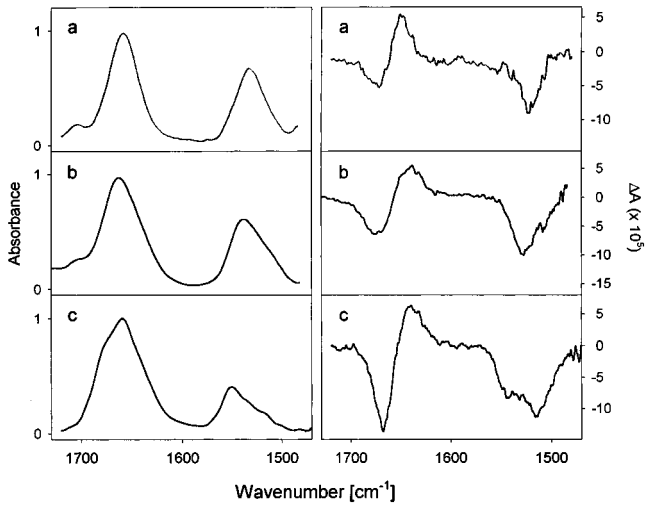

Figure 6. Experimental IR (left) and VCD (right) spectra for three model helical peptides with different fraction of α-methylated residues, measured in TFE solutions: (a) 3_{10}-helical Z-(αMe−L-Val)$_8$−OMe; (b) 3_{10}-helical Z-(Aib−Ala)$_4$−OMe; (c) α-helical Ac−(Ala$_2$−Lys-Ala$_2$)$_3$-Gly−Tyr−NH_2.

sharpening of the amide I VCD couplet, but the intensity relationship to the amide II VCD and the absorbance is maintained. The 3_{10}-helix VCD results still show a systematic shift in the balance of the amide I couplet from slightly more positive to significantly more negative as the proportion of Aib residues is decreased. The amide II VCD by contrast is stable in shape as well as intensity for both the 3_{10}-helix and α-helix. One difference does develop; the α-helix dodecamer is predicted to have an amide I IR almost twice as intense as the amide II, while except for Ac−(Aib−Ala)$_6$−NH_2 this is not true for the longer 3_{10}-helices, which tend to develop broader transitions.

The relative changes in the predicted 3_{10}-helical VCD patterns with change in Aib content of the peptide reflect characteristic experimental spectra for peptides of these helical types, examples of which are shown in Figure 5 and Figure 6. The simulated VCD spectra for Ac−Aib_4−NH_2 (Figure 1a) and, especially, Ac−Aib_{12}−NH_2 (Figure 3a) show an intensity pattern very similar to that measured for the 3_{10}-helical Z-Aib_5-L-Leu−Aib_2−OMe (Z = benzyloxycarbonyl, OMe = methoxy) as measured in $CDCl_3$ (Figure 5a)[16,17] and that measured for Z-(αMe-L-Val)$_8$−OMe in TFE (Figure 6a).[12] The change in predicted spectral shape on going to the Aib−Ala sequence Ac−(Aib−Ala)$_6$−NH_2 (Figure 3b) is reflected experimentally in the Z-(Aib-Ala)$_4$−OMe blocked peptide results in $CDCl_3$ (Figure 5b)[48,57] and in TFE (Figure 6b). The bias of the amide I couplet VCD shifts from slightly positive to more negative for the mixed peptide, and the amide II broadens so the ratio of negative amide I to amide II becomes more equivalent. The agreement between theory and experiment for relative intensity shifts and band shape changes between these two sequences is nearly quantitative, as reflected, for example, by comparing (Table 1) the experimental $\Delta A/A_{max}$ and theoretical $\Delta\epsilon/\epsilon_{max}$ values (ratios of the differential extinction coefficient to the total extinction coefficient at the amide I band maximum).

The experimental VCD spectra for the α-helical peptide $(Met_2-Leu)_6$ in $CDCl_3$ (Figure 5c)[52] show features predicted in all α-helical simulations (Figures 2 and 4) as does that for the α-helical Ala-rich peptide Ac−(AAKAA)$_3$−GY−NH_2 in TFE (Figure 6c).[29,58] The differences in the amide I band shape and relative amide I and II IR and VCD intensities from the 3_{10}-helical model spectra are again in very good agreement with the theoretical predictions. The α-helical amide I VCD couplet is more negative than the 3_{10}-helical one, but this depends on sequence. The amide II negative maximum is displaced to lower frequency from the IR maximum, though the computations underestimate the spread of these components. Comparison of $\Delta\epsilon/\epsilon_{max}$ in the simulated spectra for the α-helical Ac−Ala_{12}−NH_2 with experimental $\Delta A/A_{max}$ for α-helical peptides yields again nearly quantitative agreement (Table 1). Finally, in common with all our previous ab initio DFT peptide computations, which are necessarily for isolated, gas-phase molecules, the split between the amides I and II is overestimated as is the frequency of the amide I mode.[50]

Discussion

Comparison of Predicted 3_{10}- and α-Helical Spectra. We have previously shown that $(Ala)_n$-based α-helical peptide VCD simulations qualitatively reflect the intense amide I couplet VCD and complex negative amide II characteristic of α-helices.[25,39] Those patterns are also maintained for a range of peptide main-chain lengths both for full DFT-level calculations and for transfer onto longer peptide models. We here go the next step and compare α-helical simulated spectra for $(Aib-Ala)_n$ alternate sequences with that for all Ala sequences. The predicted band shapes for the two α-helical sequences are very similar and have only some minor quantitative variation with main-chain length. In all cases, the amide I is much more intense than the amide II, even for the ab initio calculations on the short hexapeptides, which experimentally cannot form stable α-helices. With increase in length, the amide I and II intensities coalesce into a few modes and result in sharper IR absorbance and VCD. As a result, the Ac−Ala_{12}−NH_2 predicted spectra, as well as those predicted for longer −$(Ala)_n$− peptides,[25,30,59]

(57) Keiderling, T. A. In *Infrared and Raman spectroscopy of biological materials*; Yan, B., Gremlich, H. U., Eds.; M. Dekker: New York, 1999; p 54.
(58) Yoder, G. Ph.D. Thesis, Department of Chemistry, University of Illinois at Chicago, Chicago, IL, 1997.
(59) Kubelka, J. Ph.D. Thesis, Department of Chemistry, University of Illinois at Chicago, Chicago, IL, 2002.

have almost quantitative agreement with the amide I and II IR and VCD spectra of highly α-helical (long persistence length) poly(γ-benzyl-L-glutamate).[56,60,61] This includes (1) having the maxima of the amide II IR and VCD intensity at the high- and low-wavenumber extremes, respectively, of the (exciton split) band, (2) having the negative lobe of the amide I couplet VCD more intense than the positive lobe, (3) having the amide I almost twice as intense as the amide II in IR, and (4) having the amide I VCD, most conveniently quantified by the $\Delta A/A_{max}$ ($\Delta\epsilon/\epsilon_{max}$) ratio, approximately twice as intense as the amide II VCD (Table 1).

By comparison, the 3_{10}-helical calculations have proven to be somewhat sensitive to detailed geometry and FF values, but all of our previous 3_{10}-helical Ala- or Gly-based oligopeptide results (from fully ab initio calculations) consistently yielded a weak amide I VCD of variable shape and intense negative amide II VCD.[25,39,41] The characteristic amide I positive couplet was not always evident, but the amide II was always intensely negative with various levels of computation. (In both conformations, the small feature predicted at ~1610 cm^{-1} between the amide I and II is the C-terminal primary amide deformation, which can be ignored since it would not be present in the blocked peptides we studied experimentally nor would it be significant in the aqueous solution experiments, due to H/D exchange.)

Origin of the C^{α}-Methylation-Dependent VCD Band Shape Variations. While the simulated spectra presented here for different sequences showed consistent patterns characteristic of the 3_{10}- and α-helical conformations, the C^{α}-methylation caused systematic qualitative variations in the details of the 3_{10}-helical amide I VCD band shapes. These variations are reflected by differences in the amide I normal-mode ordering and distribution of vibrations among the amide groups for particular transitions between the $-(Aib)_n-$, $-(Aib-Ala)_{n/2}-$, and $-(Ala)_n-$ sequences. Normal-mode analysis also revealed that a small admixture of the $C^{\alpha}-H$ bending motion is present as a component of the amide I vibrations for −Ala− residues. Obviously, C^{α}−methyl substitution removes this coupling by removing $C^{\alpha}-H$ from the substituted residue. In addition, in the model used here, symmetric substitution (in Aib) eliminates the chiral center at C^{α}. The differences in the VCD band shapes might be related to the intrinsic chirality of the C^{α} in Ala-based sequences sensed via the $C^{\alpha}-H$ bending mode coupling to the amide vibrations. Conversely, the possibility of mechanical coupling of $C^{\alpha}-H$ bending to the amide modes is eliminated by α-methylation in the Aib sequences. The α-methylation also causes slight changes in the backbone geometry. The $N-C^{\alpha}-C'$ valence angle in the optimized model structures is systematically smaller (by ~3°) for Aib, being on average ~111°, than for Ala (~114°). This smaller value corresponds to the experimentally determined value for Aib-based oligopeptides.[5] Such a variation can also in principle contribute to the spectral differences.

To gain some insight into the probable effect of these interactions, we performed a series of test calculations. To test for the significance of the Ala chiral center at C^{α}, ab initio calculations of the IR and VCD were carried out for $Ac-Gly_4-NH_2$ constrained to the same 3_{10}-helical ϕ, ψ, and ω dihedral angles that were used for all (−Ala-, −Aib−Ala−, and −Aib−) tetrapeptide calculations. Subsequently, isotopic substitutions for this −Gly− peptide were carried out in which specific α-hydrogens were assigned atomic masses corresponding to $-CD_3$ groups (deuterated for consistency with the $CH_3 \rightarrow CD_3$ substitution,[25,41] mass = 18.042 amu) in order to mimic the −Ala−, −Aib−Ala−, and −Aib− peptides. In the same spirit, isotopic substitutions were performed on the FF for the explicitly computed −Aib− and −Ala− tetrapeptide 3_{10}-helical models. For the −Ala− pentaamide FF, the C^{α} hydrogens were substituted with $-CD_3$ group equivalent point masses (18.042), thus mimicking the −Aib− sequence but with the Ala peptide ab initio electronic structure, including FF, APT, and AAT parameters. On the other hand, to obtain the Ala peptide with the electronic structure of the Aib one, the $Ac-Aib_4-NH_2$ FF, APT, and AAT parameters were transferred onto $Ac-Ala_4-NH_2$, with the additional Aib C^{β} parameters assigned to the $C^{\alpha}-$hydrogen. Finally, to test for the effect of the $N-C^{\alpha}-C'$ valence angle difference between −Ala− and −Aib−, we performed an ab initio calculation for $Ac-Ala_4-NH_2$ constrained to the same conformation as before, but with $N-C^{\alpha}-C'$ additionally constrained to 111°, a typical value for the Aib peptides.

The results of these tests revealed that the more intense amide I VCD computed for the Ala-containing peptides as compared to Aib cannot be attributed to the chirality of the Ala residues. The −Gly− calculations resulted in negatively biased amide I VCD similar to, and even slightly more intense than, that obtained with the −Ala− model. This is consistent with our early Hartree−Fock SCF level dipeptide results.[41,62] The isotopic substitution tests to mimic Ala and Aib led to only very small changes that were quantitatively much too small to explain the band shape variations computed with Aib → Ala change (Figure 1). Likewise, the amide I normal modes were essentially unaffected by these isotopic substitutions. Interestingly, constraining the $N-C^{\alpha}-C'$ valence angle for the Ala residues to the −Aib− value of 111° resulted in a small shift in the amide I toward lower frequency (~6 cm^{-1}), in the same direction as the amide I maximum shifted upon Ala → Aib substitution (Table 1). This frequency shift may be related to constraining the valence angle which may contribute to the high-frequency stretching/bending modes, however, no imaginary frequencies were calculated. On the other hand, the VCD band shapes remained essentially unaffected by this change in geometry. Thus, we conclude that the VCD band shape changes upon C^{α}-methylation thus arise mainly from the corresponding differences in the electronic structure, with minor contribution from the mechanical, mass-dependent coupling between the amide I and $C^{\alpha}-H$ vibrations.

We also tested for any effect of detailed variation of the conformation on the spectral band shapes. The experimentally determined 3_{10}-helical structures for the Aib-rich peptides differ slightly from those that would result from idealized 3_{10}-helices in that the average experimental α-Me 3_{10}-helical ϕ angle, based on a number of X-ray diffraction studies,[5] is around −57°. We performed an ab initio calculation on $Ac-(Aib-Ala)_4-NH_2$ constrained to $\phi = -57°$, $\psi = -30°$, and $\omega = 180°$. The differences in the resulting simulated spectra from that of the idealized structure with $\phi = -60°$ are small, as we had expected;

(60) Singh, R. D.; Keiderling, T. A. *Biopolymers* **1981**, *20*, 237.
(61) Lal, B. B.; Nafie, L. A. *Biopolymers* **1982**, *21*, 2161.
(62) Bour, P. Ph.D. Thesis, Academy of Science of the Czech Republic, Prague, Czech Republic, 1993.

however, a decrease in the amide I VCD intensity is predicted, thus providing an even slightly better correspondence to experiment (Figure 5) for the experimental structure.

Spectral Discrimination of 3_{10}-Helices. All of our theoretically based evidence suggests that VCD is not affected on a qualitative basis by residue type, proteinic versus $C^{\alpha,\alpha}$-dialkylated α-amino acid, or by peptide main-chain length. These computations predict that there is some effect of Aib on the details of the VCD band shape but demonstrate clearly that residue type is clearly not the dominant source of the difference between 3_{10}- and α-helical characteristic patterns, which centers on the overall relative intensity of the amide I and II VCD bands. This conclusion is consistent with a body of experimental data that shows consistent α-helical VCD patterns for proteins and peptides having any sequence[29,55,56,60,63−65] and suggests consistent 3_{10}-helical VCD patterns for several 3_{10}-helical peptides containing varying amounts of C^{α}-methylated residues.[12,16,17,51] Furthermore, any of the usual blocking groups do not adversely affect VCD spectra, in contrast to their common interference in ECD spectral analyses. The key to this stability of the VCD spectra−structure correlation is its reliance on relative band shapes as opposed to absolute signal size or precise frequencies, both of which are affected by solvent and disorder, and its dependence on relatively local, short-range interactions between residues.[17,42−44]

Our ab initio DFT force field calculations result in amide I frequencies that are systematically too high (Table 1), which, as we have shown,[50] can be corrected by inclusion of solvent effects. No direct connection between these absolute calculated frequencies and those observed in solution can thus be drawn. The effect of the solvent on the vibrational frequencies may depend on Aib substitution, for example, due to the excluded volume of the additional methyl groups. Likewise 3_{10}- and α-helical structures may be affected differently, in the simplest approximation, due to different overall dipole moments of the two structures. The relative frequencies observed in solution may thus be different from relative frequencies predicted in the isolated molecule simulation, and the frequency assignments may be further complicated by these sequence- and conformation-sensitive solvent effects. However, the relative frequency changes predicted in our calculations are inherent to the variations in sequence, length, and conformation and as such provide a useful picture of these effects on vibrational frequencies in the absence of solvent perturbation. For example, while the amide I frequencies in α-helices are predicted to be systematically higher than the 3_{10}-helical ones for the same sequence (Table 1), the α-helical IR amide I consistently shows a sideband toward lower frequency (Figures 2 and 4), which is at approximately the same position as the corresponding 3_{10}-helical maximum. Such a sideband has been observed in the spectra of some helical proteins[18,19,31,33,66] and attributed to distorted α-helix or 3_{10}-helix. However, as suggested by Torii and Tasumi,[22] based on the empirical coupled oscillator model, and Krimm and co-workers,[23,67] based on empirical force field calculations, these may be actually due to end effects in finite, regular helices. This is confirmed in our ab initio α-helical calculations where such a band also appears in the simulated spectra arising mainly due to the N-terminal amide group, which makes it relatively less apparent in simulated spectra for longer peptides. Interestingly, while the 3_{10}-helical models also have their lowest frequency amide I mode associated with the N-terminal amide vibrations, these are much closer in frequency to the central modes and do not result in a resolved sideband on the amide I spectrum (Figure 1, 3).

On the other hand, the predicted VCD band shapes remain qualitatively the same for a particular conformation and do not change significantly due to nonstereochemical effects, such as solvent interaction. Although it is not a priori clear, as a reviewer has pointed out, that frequency shifts on the order of several tens of wavenumbers would not change the VCD band shapes arising from splittings between particular normal modes on the order of 1 cm^{-1}, this stability has been confirmed by our test calculations that include solvent on various levels. Tests with the implicit solvent model (conductor polarized continuum model, CPCM)[68,69] to model a polar, but non-hydrogen-bonding solvent, such as acetonitrile, showed that the vibrational frequency of the 3_{10}-helical Aib−Ala sequence shifted less than that of the all-Ala sequence, resulting in approximately the same amide I (∼1677 cm^{-1}) as well as amide II (∼1510 cm^{-1}) frequencies for both. By contrast, the VCD patterns remain constant and essentially identical to those presented in Figure 1. In addition, in our latest computational studies[59] on oligopeptides with explicitly hydrogen-bonded water molecules, while the amide frequencies shift substantially closer to the aqueous solution experimental values, the normal mode ordering and the VCD band shapes remain essentially the same. All these computational results are therefore consistent with both the good agreement between the experimental VCD band shapes in solution and isolated molecule computational results[25,30,39] and with the experimental evidence that the VCD band shapes remain stable as long as the conformation is the same, even though the vibrational frequencies can shift considerably, for example, in different solvents.[12,29,48]

Since theory and experiment agree, it is worth trying to explain from where this stability of VCD shape arises. The basic property affecting the amide I frequency is the C═O bond strength which is reflected in its length. Solvent-corrected theoretical results tend to lengthen the C═O bond and reduce its vibrational frequency.[50] Coupling of these local modes is not affected to first order by their frequency; thus, the splitting patterns are relatively stable. (It is assumed that all the local modes will have an equivalent solvent shift in a uniform structure.) VCD is a stereochemical phenomenon whose intensities result from these couplings as well as through-space dipolar interactions.[25] These again are not impacted to first order by changes in local oscillator frequencies. Thus, VCD gains band shape stability under conditions leading to frequency shifts.

Suggestions of very large H/D exchange effects on the 3_{10}-helical amide I/I′ frequency as compared to the α-helix have appeared based on IR spectra of peptides[35,36] and proteins[20] in D_2O solution. Our simulations show that H/D exchange alone shifts both the α-helical and 3_{10}-helical amide I down by ∼4−5

(63) Yasui, S. C.; Keiderling, T. A. *J. Am. Chem. Soc.* **1986**, *108*, 5576.
(64) Baumruk, V.; Keiderling, T. A. *J. Am. Chem. Soc.* **1993**, *115*, 6939.
(65) Baumruk, V.; Pancoska, P.; Keiderling, T. A. *J. Mol. Biol.* **1996**, *259*, 774.
(66) Haris, P. I. In *Infrared Analysis of Peptides and Proteins: Principles and Applications*; ACS Symposium Series 750; Ram Singh, B., Ed.; American Chemical Society: Washington, DC, 2000; p 54.
(67) Krimm, S. In *Infrared Analysis of Peptides and Proteins: Principles and Applications*; ACS Symposium Series 750; Singh, B. R., Ed.; American Chemical Society: Washington, DC, 2000; p 38.
(68) Klamt, A.; Schuurmann, G. *J. Chem. Soc., Perkin Trans.* **1993**, *2*, 799.
(69) Barone, V.; Cossi, M. *J. Phys. Chem.* **1998**, *102*, 1995.

cm^{-1}. Experimentally, model 3_{10}-helical compounds (e.g., Aib_5−L-Leu−Aib_2 and $(Aib-L\text{-}Ala)_4$)[59,70] show a shift of ∼5−6 cm^{-1} for the amide I/I′ on H/D exchange (both measured in $CDCl_3$), which is the same as seen for the α-helical model oligopeptides.[29] Protein α-helices exhibit the same ∼4−5 cm^{-1} shift in the amide I frequency in D_2O. None of these results thus supports a large shift for 3_{10}-helices upon deuteration. By contrast, isolated α-helices in water and D_2O do have amide I frequencies sharply shifted from their nonaqueous solution values.[29,58] Solvation effects thus obscure the utility of the frequency shifts for conformational studies and remain the only potential explanation for the sharply low-frequency modes assigned to 3_{10}-helices, aside from error. As a consequence, these purported frequency assignments cannot be considered characteristic for the 3_{10}-helical conformation, since buried or only partially solvated helices would have higher amide I′ frequencies.

In summary, amide I frequencies provide an indecisive structural signature (small shift upon structural change) which is as much dependent on the details of oligopeptide sequence and length as on the conformation. The small differences in frequency are probably at the reliability limits of our calculations even in a relative sense. If the complete neglect of solvent and structural irregularities in the calculations are taken into account, it is very unlikely that any inherent, conformation-specific amide I vibrational frequencies can be assigned to differentiate between α- or 3_{10}-helices.

Conclusion

Ab initio-based simulations of IR and VCD spectra on model 3_{10}- and α-helical peptides explicitly containing α-methylated residues showed that the α-methylation does have an effect on the details of VCD band shapes. This effect, which arises primarily from the perturbation of the electronic distribution due to the extra α-methyl group, decreases the intensity of the amide I VCD and makes it a more conservative couplet. Both 3_{10}- and α-helical spectra were altered by the α-methylation, but the changes were significantly smaller for α-helices. Nevertheless, all 3_{10}-helical models, independent of the fraction of α-methylated residues, have a pattern in amide I and II VCD intensities distinct from the α-helical model peptides, both with and without α-methylation. VCD thus provides a direct means for distinguishing these two helical conformations if both the amides I and II can be measured. The IR absorption, on the other hand, exhibits small frequency shifts that are dependent on both the conformation and α-methylation. Much larger effects on the vibrational frequencies can be expected due to the environment, such as burial in protein interior or exposure to solvent. Such solvent effects on IR and VCD spectra of peptides are the subject of a future paper. The amide I frequency shifts upon H/D exchange are predicted to be the same for both α- and 3_{10}-helical structures, in agreement with experimental data. The reported large amide I low-frequency shift upon N-deuteration for 3_{10}-helix is thus not supported.

Acknowledgment. This work was funded in part by a grant from the Petroleum Research Fund administered by the American Chemical Society. J.K. was supported as a UIC Dean's Scholar for part of this project. We thank Claudio Toniolo, Fernando Formaggio, Ryoichi Katachai, and Andre Brack for peptide samples, Sritana Yasui, Qi Xu, Gorm Yoder, and Dongfang Huo for obtaining some of the experimental data, and a reviewer for insightful comments.

JA012685O

(70) Huo, D.; Keiderling, T. A. Unpublished.